Dynamic analysis of a tire using a nonlinear Timoshenko ring model

Trong-Dai Vu, Denis Duhamel, Zouhir Abbadi, Yin Hai-Ping, Arnaud Gaudin

Dynamic analysis of a tire using a nonlinear Timoshenko ring model

T. D. Vu [1,2], **D. Duhamel** [1], **Z. Abbadi** [2], **H.P. Yin** [1], **A. Gaudin** [2]
[1] Université Paris-Est, Laboratoire Navier,
ENPC-IFSTTAR-CNRS,UMR 8205,
Ecole des Ponts ParisTech,
6 et 8, Avenue Blaise Pascal - Cité Descartes, Champs-sur-Marne
77455 Marne La Vallée Cedex 2, France
Email: vutro@enpc.fr

[2] PSA Peugeot Citroën, Automotive Research and Advanced Engineering Division,
Centre Technique de Vélizy A
Route de Gisy 78943 - Case courrier vv1415
78943 Vélizy-Villacoublay, France

Abstract
It is well known that tires play an important role in the generation of rolling noise. For low frequencies, the circular ring model can describe in a simple way the tire dynamic behaviour. This model is based on the Euler Bernoulli beam theory and takes into account the prestress generated by the internal air pressure but is otherwise linear. However, nonlinear effects resulting from high internal pressure and vehicle load can be important. In particular, vehicle load generates contact forces and a non-circular geometry in stationary rolling conditions.This paper presents a nonlinear flexible ring model based on the Timoshenko beam theory. It is used to simulate the nonlinear static deformation of a tire resulting from the application of vehicle load and inflation pressure. It is also applied to study the effect of these two parameters on the dynamic behaviour of the tire around its nonlinear static state by computing normal modes and transfer functions. In both static and dynamic cases, the results are in good agreement with Abaqus simulations considered as reference.

1 Introduction

In the automotive industry, interior rolling noise represents one of the main NVH issues. Briefly, it is a broadband noise resulting from the contact of tires with a rough surface. The tire/road contact excitations are transmitted into the cabin taking two transmission paths:

- Solid transmission path through tires, wheels, suspensions and the car body. It results in the so called structure-borne noise and represents the dominant contribution up to 400Hz.
- Aerial transmission path through panels. This generates the airborne noise and is the major source in the medium and high frequency bands.

Analytical models, which can describe in a simple way the tire behaviour in the low frequency band, exist in the literature. We find simple 2D ring models, introduced a long time ago [1], and somewhat more complex 3D plate models [6] and 3D shell models [4] [5]. As we know, 2D ring models, including Böhm model, are based on the Euler Bernoulli beam theory and take into account the prestress generated by the internal air

pressure but are otherwise linear. This work is a development of an analytical 2D ring model allowing the investigation of the nonlinear effects on the dynamic behaviour of tires under internal pressure and vehicle load.

This paper begins with a detailed presentation of the proposed model. The assumptions used in its construction are exposed and the analytical formulations of the equilibrium equations are established. The specific developments relating to the nonlinear model are highlighted relatively to the existing literature [3]. Then, the full nonlinear numerical resolution using Matlab is presented. It is followed by the validation of the model based on comparisons with Abaqus simulations considered as reference: deformed shapes in the static case, eigenmodes and transfer functions in the dynamic case. This is achieved for both Euler Bernoulli and Timoshenko beams in order to analyse the difference between the two formulations.

2 Description of the model

The proposed tire model is a 2D ring model. The treadband is modelled with a circular beam. The sidewalls are represented by radial and tangential springs. The following assumptions are considered:

- The ring radius is large compared with the dimensions of the cross section.
- The ring consists of Cosserat-Timoshenko beams. The shear effect is taken into account and there is no warping of the cross section.
- The surface of the cross section does not change after being deformed.
- The material of the beam is linear elastic and isotropic.

Moreover, finite transformations defined by large displacements and small deformations are assumed. In this way, the proposed model will be able to take into account the nonlinear deformations arising from inflation pressure and road contact forces generated by vehicle load.

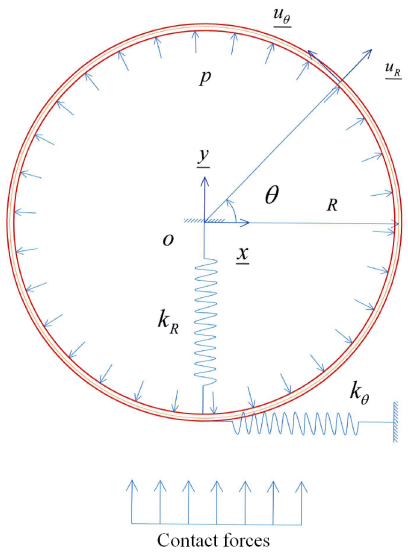

Figure 1: Illustration of the ring model

2.1 The kinematic of the model

Each material point in the initial configuration is defined by two coordinates (z, θ) in the polar system $(\underline{u}_R, \underline{u}_\theta)$. The variable z is in the range $[-\frac{e}{2}, \frac{e}{2}]$ and θ is in the range $[0, 2\pi]$. It is assumed that all quantities depend only on the variable θ.
Thus, the position of any material point, P_0, in the initial configuration of the ring cross section can be written as follows:

$$\underline{OP_0} = \underline{OS_0} + \underline{S_0P_0} = (R + z)\underline{u_R} \tag{1}$$

where O is the centre of the ring and S_0 is located on the neutral axis of the section. To switch to the current configuration, the point S_0 moves to S by two translations $u(\theta)$ and $w(\theta)$ and the point P_0 rotates by an angle $\alpha(\theta)$ to become the point P. Therefore, the transformation of the material vector in the current frame is defined by:

$$\underline{OP} = \underline{OS} + \underline{SP} = (R + u + z\cos\alpha)\underline{u_R} + (w + z\sin\alpha)\underline{u_\theta} \tag{2}$$

Each point of the ring is then entirely defined by the degrees of freedom triplet: (u, w, α).
Using the equations (1) and (2), the displacement vector of material points can be written:

$$\underline{u} = \underline{OP} - \underline{OP_0} = (u + z(\cos\alpha - 1))\underline{u_R} + (w + z\sin\alpha)\underline{u_\theta} \tag{3}$$

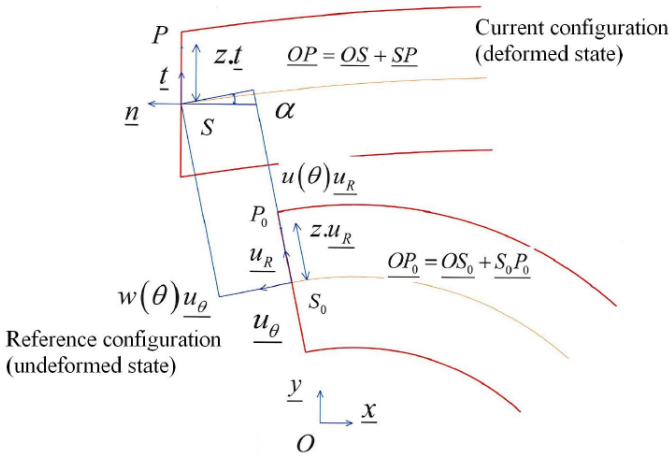

Figure 2: Kinematic of the proposed model

The gradient of transformation tensor is:

$$\underline{\underline{F}} = \frac{d\underline{OP}}{d\underline{OP_0}} = \begin{pmatrix} \cos\alpha & \frac{1}{R+z}(u' - w - z(\alpha' + 1)\sin\alpha) \\ \sin\alpha & \frac{1}{R+z}(R + u + w' + z(\alpha' + 1)\cos\alpha) \end{pmatrix} \tag{4}$$

where, the prime stands for the partial derivation regarding θ.
We deduce the tensor of the deformation:

$$\underline{\underline{e}} = \frac{1}{2}(\underline{\underline{F}}.\underline{\underline{F}}^T - \underline{\underline{1}}) = \begin{pmatrix} e_{RR} & e_{R\theta} \\ e_{\theta R} & e_{\theta\theta} \end{pmatrix} \tag{5}$$

$$\begin{cases} e_{RR} = 0 \\ e_{R\theta} = e_{\theta R} = \frac{(\zeta^2 - \zeta + 1)((u' - w)\cos\alpha + (R + u(\theta) + w'(\theta))\sin\alpha)}{2R} \\ e_{\theta\theta} = \frac{1}{2}\left(\begin{array}{l} \frac{(\zeta^2 + \zeta + 1)^2(R\zeta(\alpha' + 1)\cos\alpha + R + u + w')^2}{R^2} \\ + \frac{(\zeta^2 - \zeta + 1)^2(R\zeta(\alpha' + 1)\sin\alpha + w - u')^2}{R^2} - 1 \end{array} \right) \end{cases} \tag{6}$$

with $\zeta = \frac{z}{R}$. In fact, it is assumed that the material behaviour of the ring is linear. Therefore, the stress field which is calculated by a product between the doubly contracted tensor of the deformation and the stiffness tensor can be written in engineering notation:

$$\begin{pmatrix} \sigma_{\theta\theta} \\ \sigma_{R\theta} \end{pmatrix} = \begin{pmatrix} E & 0 \\ 0 & G \end{pmatrix} \begin{pmatrix} e_{\theta\theta} \\ 2e_{R\theta} \end{pmatrix} \tag{7}$$

where E and G are respectively the Young and shear modulus of the constitutive material of the ring. Activated forces on the cross-section are the normal force N, the shear force V and the moment M in the current frame $(\underline{t}, \underline{n})$ which is calculated as follows:

$$\begin{cases} N = \int\limits_A \sigma_{\theta\theta} dA = \int\limits_A E.e_{\theta\theta} dA = \left(-\frac{EI}{R^2}\left((\alpha'+1)\cos\alpha - \frac{R+u+w'}{R}\right)\frac{R+u+w'}{R}\right. \\ \quad + \frac{EI}{R^2}\left((\alpha'+1)\sin\alpha + \frac{u'-w}{R}\right)\frac{u'-w}{R} + \frac{1}{2}\frac{EA}{R^2}\left((w-u')^2 + (R+u+w')^2 - R^2\right) \\ \quad \left. + \frac{1}{2}\frac{EI}{R^2}\left((\alpha'+1)\sin\alpha + \frac{u'-w}{R}\right)^2 + \frac{1}{2}\frac{EI}{R^2}\left((\alpha'+1)\cos\alpha - \frac{R+u+w'}{R}\right)^2\right) \\ V = \int\limits_A \sigma_{R\theta} dA = \int\limits_A G.2e_{R\theta} dA = \left(\frac{GA}{R} + \frac{GI}{R^3}\right)\left((u'-w)\cos\alpha + (R+u+w')\sin\alpha\right) \\ M = \int\limits_A z.\sigma_{\theta\theta} dA = \int\limits_A E.ze_{\theta\theta} dA = \frac{EI}{R}\left(\frac{R+u+w'}{R}\left((\alpha'+1)\cos\alpha - \frac{R+u+w'}{R}\right)\right. \\ \quad \left. - \frac{u'-w}{R}\left((\alpha'+1)\sin\alpha + \frac{u'-w}{R}\right)\right) \end{cases} \tag{8}$$

where A is the cross section area and I the cross section moment of inertia.

2.2 Static equilibrium equations

We use the 2D equilibrium equations of beam established by F. Davi [2], J. C. Simo [7] [8] in the current configuration:

$$\begin{cases} \frac{\partial \underline{f}}{\partial s} + \underline{q} = 0 \\ \frac{\partial M}{\partial s} + \frac{\partial OS}{\partial s} \wedge \underline{f} + g = 0 \end{cases} \tag{9}$$

where s is the curvilinear abscissa in the reference configuration which can be expressed as a function of θ by $ds = Rd\theta$, and $\underline{x} \wedge \underline{y}$ denotes the cross product of the vectors $\underline{x}$ and $\underline{y}$.

$\underline{f} = \begin{pmatrix} V \\ N \end{pmatrix}$ and M are respectively the activated forces and moment on the cross section.

$\underline{q} = \oint\limits_{\partial A} \underline{q^s} dl + \int\limits_A \underline{q^v}.dA$ is the sum of surface forces $\underline{q^s}$ and volume forces $\underline{q^v}$ applied on the beam. It includes in our problem the inflating pressure $\underline{p}$ represented by a uniformly distributed load on the whole ring, the radial and tangential spring forces $\underline{F^{spr}_{rad}}$ and $\underline{F^{spr}_{tan}}$, the contact forces $\underline{f_R}$ assumed to be always in the radial direction.

The sum of the moments applied along the beam, g, is equal to zero in our problem.

To move from the current configuration to the reference configuration, we introduce the $\underline{\underline{\Gamma(\theta)}}$ transition matrix:

$$\begin{pmatrix} \underline{t} \\ \underline{n} \end{pmatrix} = \begin{pmatrix} \cos\alpha & \sin\alpha \\ -\sin\alpha & \cos\alpha \end{pmatrix} \begin{pmatrix} \underline{u_R} \\ \underline{u_\theta} \end{pmatrix} = \underline{\underline{\Gamma(\theta)}} \begin{pmatrix} \underline{u_R} \\ \underline{u_\theta} \end{pmatrix} \tag{10}$$

The equilibrium equations are written in the reference configuration as follows:

$$\begin{cases} \frac{1}{R}\frac{d}{d\theta}\left(\underline{\underline{\Gamma(\theta)}}\begin{pmatrix} V \\ N \end{pmatrix}\right) + \underline{p} + \underline{f_R} + \underline{F^{spr}_{rad}} + \underline{F^{spr}_{tan}} = 0 \\ \frac{1}{R}\frac{dM}{d\theta} + \frac{1}{R}\frac{\partial OS'}{\partial \theta} \wedge \underline{\underline{\Gamma(\theta)}}\begin{pmatrix} V \\ N \end{pmatrix} = 0 \end{cases} \tag{11}$$

2.2.1 Linear case

In the linear case, all the second order terms are neglected. Consequently, the activated forces and moment in the cross section become:

$$N = EA\frac{u+w'}{R} + \frac{EI}{R^2}\left(\frac{u+w'}{R} - \alpha'\right) \ , \quad V = \left(GA + \frac{GI}{R^2}\right)\left(\frac{u'-w}{R} + \alpha\right) \ , \quad M = \frac{EI}{R}\left(\alpha' - \frac{u+w'}{R}\right) \tag{12}$$

Besides, the exterior forces applied in the model are written in a simple manner as follows:

$$\underline{p} = p\underline{u_R} \ , \qquad \underline{F_{rad}^{spr}} = k_R u\underline{u_R} \ , \qquad \underline{F_{tan}^{spr}} = k_\theta w\underline{u_\theta} \ , \qquad \underline{f_R} = f_R\underline{u_R} \tag{13}$$

where k_R and k_θ are respectively the stiffness of the radial and tangential springs.
We apply the relations (12) and (13) to the general equation (11) and we consider that the deformed and undeformed configurations are confounded (the transition matrix becomes the identity). Finally, the equilibrium equations of Timoshenko's beam are thus written:

$$\left\{\begin{array}{l} \left(\frac{GA}{R} + \frac{GI}{R^3}\right)\left(\frac{u''-w'}{R} + \alpha'\right) - \frac{EA}{R}\left(\frac{u+w'}{R}\right) - \frac{EI}{R^3}\left(\frac{u+w'}{R} - \alpha'\right) + p + f_R - k_R u = 0 \\ \frac{EA}{R}\left(\frac{u'+w''}{R}\right) + \frac{EI}{R^3}\left(\frac{u'+w''}{R} - \alpha''\right) + \left(\frac{GA}{R} + \frac{GI}{R^3}\right)\left(\frac{u'-w}{R} + \alpha\right) - k_\theta w = 0 \\ \frac{EI}{R^2}\left(\alpha'' - \frac{u'+w''}{R}\right) - GA\left(\frac{u'-w}{R} + \alpha\right) = 0 \end{array}\right. \tag{14}$$

The case of Euler Bernoulli's beam is obtained from the more general case of Timoshenko beam. In this case the shear deformation vanishes so the shear modulus tends to infinity. The relation between the rotation angle α of the cross section and the displacements u and w is established as follows:

$$\left\{\begin{array}{l} G \to \infty \\ e_{R\theta} \to 0 \end{array}\right. \Leftrightarrow \left\{\begin{array}{l} G \to \infty \\ (u'-w)\cos\alpha + (R+u+w')\sin\alpha \to 0 \end{array}\right. \Rightarrow \alpha \cong \tan\alpha = \frac{w-u'}{R+u+w'} \cong \frac{w-u'}{R} \tag{15}$$

We use this relation for writing the equilibrium equations of Euler Bernoulli's beam:

$$\left\{\begin{array}{l} -\frac{EA}{R^2}(w'+u) - \frac{EI}{R^4}(u+u'') - \frac{EI}{R^4}(u''''+u'') + p - f_R - k_R u = 0 \\ \frac{EA}{R^2}(w''+u') - k_\theta w = 0 \end{array}\right. \tag{16}$$

2.2.2 Case with geometric nonlinearities

In the case of geometric nonlinearities, the air pressure, the radial and tangential springs follow the displacement of the ring. This is expressed as follows:

$$\begin{array}{ll} \underline{p} = p\underline{Oz} \wedge \frac{\partial \underline{OS'}}{\partial s} = p\underline{Oz} \wedge \frac{\partial \underline{OS'}}{R\partial\theta} \ , & \underline{F_{rad}^{spr}} = k_R u\underline{Oz} \wedge \frac{\partial \underline{OS'}}{\partial s} = k_R u\underline{Oz} \wedge \frac{\partial \underline{OS'}}{R\partial\theta} \\ \underline{F_{tan}^{spr}} = k_\theta w\frac{\partial \underline{OS'}}{\partial s} = k_\theta w\frac{\partial \underline{OS'}}{R\partial\theta} \ , & \underline{f_R} = f_R\underline{u_R} \end{array} \tag{17}$$

leading to the equilibrium equations:

$$\left\{\begin{array}{l} \frac{1}{R}\left(V'\cos\alpha - N'\sin\alpha - (\alpha'+1)(V\sin\alpha + N\cos\alpha)\right) + p\left(\frac{R+u+w'}{R}\right) \\ \qquad + f_R - k_R u\left(\frac{R+u+w'}{R}\right) - k_\theta w\left(\frac{u'-w}{R}\right) = 0 \\ \frac{1}{R}\left(V'\sin\alpha + N'\cos\alpha + (\alpha'+1)(V\cos\alpha - N\sin\alpha)\right) - p\left(\frac{u'-w}{R}\right) \\ \qquad + k_R u\left(\frac{u'-w}{R}\right) - k_\theta w\left(\frac{R+u+w'}{R}\right) = 0 \\ \frac{1}{R}M' + \frac{1}{R}\left((u'-w)(V\sin\alpha + N\cos\alpha) - (R+u+w')(V\cos\alpha - N\sin\alpha)\right) = 0 \end{array}\right. \tag{18}$$

where (M, N, V) are defined by the formulas (8).
The system (18) consists of three nonlinear ordinary differential equations with the variables (u, w, α). The resolution of this set of equations cannot be achieved analytically. A numerical method for solving this system is presented in part 3.1.

2.3 Dynamic equilibrium equations

The dynamic equilibrium equations are established around the static equilibrium state. Small perturbations are added to the static displacements as follows:

$$u + u_t(t,\theta)\ , \qquad w + w_t(t,\theta)\ , \qquad \alpha + \alpha_t(t,\theta) \tag{19}$$

with $\frac{u_t}{R} \ll 1$, $\frac{w_t}{R} \ll 1$ and $\frac{\alpha_t}{R} \ll 1$.
(u, w, α) and (M, N, V) being determined in static step, the resolution of the dynamic system consists in finding (u_t, w_t, α_t).

2.3.1 Case of linear static displacement

The equations of the vibrations of Timoshenko's beam are obtained by introducing the equations (19) into the linear static equilibrium equations (14) and adding acceleration terms in each equation:

$$\left\{\begin{array}{l} \left(\frac{GA}{R}+\frac{GI}{R^3}\right)\left(\frac{{u_t}''-{w_t}'}{R}+{\alpha_t}'\right)-\frac{EA}{R}\left(\frac{u_t+{w_t}'}{R}\right)-\frac{EI}{R^3}\left(\frac{u_t+{w_t}'}{R}-{\alpha'}_t\right)+f_R^t-k_R u_t=\rho A\ddot{u}_t \\ \frac{EA}{R}\left(\frac{{u_t}'+{w_t}''}{R}\right)+\frac{EI}{R^3}\left(\frac{{u_t}'+{w_t}''}{R}-{\alpha_t}''\right)+\left(\frac{GA}{R}+\frac{GI}{R^3}\right)\left(\frac{{u_t}'-w_t}{R}+\alpha_t\right)-k_\theta w_t=\rho A\ddot{w}_t \\ \frac{EI}{R^2}\left({\alpha_t}''-\frac{{u_t}'+{w_t}''}{R}\right)-\left(GA+\frac{GI}{R^2}\right)\left(\frac{{u_t}'-w_t}{R}+\alpha_t\right)=\rho I\ddot{\alpha}_t \end{array}\right. \tag{20}$$

where f_R^t is the dynamic excitation force applied on the basis of the deformed tire.
The equations of the vibrations of Euler Bernoulli's beam can also be written as:

$$\left\{\begin{array}{l} -\frac{EA}{R^2}\left({w_t}'+u_t\right)-\frac{EI}{R^4}\left(u_t+{u_t}''\right)-\frac{EI}{R^4}\left({u_t}''''+{u_t}''\right)+p_t-f_R^t-k_R u_t=\rho A\ddot{u}_t \\ \frac{EA}{R^2}\left({w_t}''+{u_t}'\right)-k_\theta w_t=\rho A\ddot{w}_t \end{array}\right. \tag{21}$$

2.3.2 Case of a static displacement with geometric nonlinearities

Considering the nonlinear displacement of the static state, the dynamics equations are:

$$\left\{\begin{array}{l} \frac{1}{R}\left(-\alpha_t V'\sin\alpha-\alpha_t N'\cos\alpha+{V_t}'\cos\alpha-{N_t}'\sin\alpha+{\alpha_t}'\left(-V\sin\alpha-N\cos\alpha\right)\right. \\ \left.-\left(\alpha'+1\right)\left(V_t\sin\alpha+N_t\cos\alpha+\alpha_t V\cos\alpha-\alpha_t N\sin\alpha\right)\right)-k_R u_t\left(\frac{R+u+{w}'}{R}\right)+f_R^t \\ -k_\theta w_t\left(\frac{u'-w}{R}\right)+p\left(\frac{u_t+{w_t}'}{R}\right)-k_R u\left(\frac{u_t+{w_t}'}{R}\right)-k_\theta w\left(\frac{{u_t}'-w_t}{R}\right)=\rho A\ddot{u}_t \\ \frac{1}{R}\left(\alpha_t V'\cos\alpha-\alpha_t N'\sin\alpha+{V_t}'\sin\alpha+{N_t}'\cos\alpha+{\alpha_t}'\left(V\cos\alpha+N\sin\alpha\right)\right. \\ \left.+\left(1+\alpha'\right)\left(V_t\cos\alpha-N_t\sin\alpha\right)-\alpha_t V\sin\alpha-\alpha_t N\cos\alpha\right)-p\left(\frac{{u_t}'-w_t}{R}\right)+k_R u\left(\frac{{u_t}'-w_t}{R}\right) \\ +k_R u_t\left(\frac{u'-w}{R}\right)-k_\theta w\left(\frac{u_t+{w_t}'}{R}\right)-k_\theta w_t\left(\frac{R+u+{w}'}{R}\right)=\rho A\ddot{w}_t \\ \frac{1}{R}{M_t}'+\frac{1}{R}\left(\left({u_t}'-w_t\right)\left(V\sin\alpha+N\cos\alpha\right)-\left(u_t+{w_t}'\right)\left(V\cos\alpha-N\sin\alpha\right)\right. \\ +\left({u_s}'-{w_s}\right)\left(\alpha_t V\cos\alpha-\alpha_t N\sin\alpha\right)-\left(R+u+{w}'\right)\left(-\alpha_t V\sin\alpha-\alpha_t N\cos\alpha\right) \\ \left.+\left(u'-w\right)\left(V_t\sin\alpha+N_t\cos\alpha\right)-\left(R+u+{w}'\right)\left(V_t\cos\alpha-N_t\sin\alpha\right)\right)=\rho I\ddot{\alpha}_t \end{array}\right. \tag{22}$$

where:

$$M_t=\frac{EI}{R}\left(\begin{array}{l} \left(\frac{u_t+{w_t}'}{R}\right)\left(\left(1+\alpha'\right)\cos\alpha-\frac{R+u+{w}'}{R}\right) \\ +\left(\frac{{u_t}'-w_t}{R}\right)\left(\left(1+\alpha'\right)\sin\alpha+\frac{u'-w}{R}\right)+\left(\frac{u'-w}{R}\right) \\ +\left(\frac{R+u+{w}'}{R}\right)\left({\alpha_t}'\cos\alpha-\left(1+\alpha'\right)\alpha_t\sin\alpha-\frac{u_t+{w_t}'}{R}\right) \\ +\left(\frac{u'-w}{R}\right)\left({\alpha_t}'\sin\alpha+\left(1+\alpha'\right)\alpha_t\cos\alpha+\frac{{u_t}'-w_t}{R}\right) \end{array}\right)$$

$$V_t=\left(\frac{GA}{R}+\frac{GA}{R^3}\right)\left(\begin{array}{l} \left({u_t}'-w_t\right)\cos\alpha-\left(u'-w\right)\alpha_t\sin\alpha \\ +\left(R+u+{w}'\right)\alpha_t\cos\alpha+\left(u_t+{w_t}'\right)\sin\alpha \end{array}\right)$$

$$\mathrm{N}_t = \begin{pmatrix} \frac{EA}{R^2}\left((u'-w)\left(u_t{}'-w_t\right)+\left(u+w'\right)\left(u_t+w_t{}'\right)\right)+\frac{EA}{R}\left(u_t+w_t{}'\right) \\ +\frac{EI}{R^2}\left(\alpha'_t\sin\alpha+\left(1+\alpha'\right)\alpha_t\cos\alpha+\frac{u'_t-w_t}{R}\right)\frac{u'-w}{R} \\ -\frac{EI}{R^2}\left(\alpha'_t\cos\alpha-\left(1+\alpha'\right)\alpha_t\sin\alpha-\frac{u_t+w'_t}{R}\right)\frac{R+u+w'}{R} \\ +\frac{EI}{R^2}\left(\left(1+\alpha'\right)\sin\alpha+\frac{u'-w}{R}\right)\left(\alpha'_t\sin\alpha+\left(1+\alpha'\right)\alpha_t\cos\alpha+\frac{u'_t-w_t}{R}\right) \\ +\frac{EI}{R^2}\left(\left(1+\alpha'\right)\cos\alpha-\frac{R+u+w'}{R}\right)\left(\alpha'_t\cos\alpha-\left(1+\alpha'\right)\alpha_t\sin\alpha-\frac{u_t+w'_t}{R}\right) \\ +\frac{EI}{R^2}\left(\left(1+\alpha'\right)\sin\alpha+\frac{u'-w}{R}\right)\frac{u'_t-w_t}{R}-\frac{EI}{R^2}\left(\left(1+\alpha'\right)\cos\alpha-\frac{R+u+w'}{R}\right)\frac{u_t+w'_t}{R} \end{pmatrix}$$

Since the equations (22) are linear with the unknown vector $\underline{u_t} = (u_t, w_t, \alpha_t)$, they can be rewritten in the following simple form:

$$\underline{\underline{K}}\,\underline{u_t} + \underline{\underline{M}}\,\underline{\ddot{u}_t} = \underline{f_R^t} \tag{23}$$

where $\underline{\underline{K}}$ and $\underline{\underline{M}}$ are the mass and tangent stiffness matrices resulting from the static step and $\underline{f_R^t} = \begin{pmatrix} f_R^t \\ 0 \\ 0 \end{pmatrix}$

3 Numerical implementation

The numerical resolution of (18), for example, consists of solving ordinary differential equations of second order with periodic conditions:

$$\begin{cases} \underline{u}\,(\theta) = f(\theta, \underline{u}, \underline{u}') \\ \underline{u}(0) = \underline{u}(2\pi) \\ \underline{u}'(0) = \underline{u}'(2\pi) \\ \theta \in [0, 2\pi] \end{cases} \tag{24}$$

We use the finite difference method. A mesh with N points, $\theta_i = (\frac{2\pi(i-1)}{N})_{i=1\ldots N}$, is considered. The discretization scheme is written as follows:

$$\begin{cases} \underline{u}'(\theta_i) \cong \frac{\underline{u}(\theta_{i+1})-\underline{u}(\theta_{i-1})}{2h} = \frac{\underline{u}_{i+1}-\underline{u}_{i-1}}{2h} \\ \underline{u}''(\theta_i) \cong \frac{\underline{u}(\theta_{i+1})-2\underline{u}(\theta_i)+\underline{u}(\theta_{i-1})}{h^2} = \frac{\underline{u}_{i+1}-2\underline{u}_i+\underline{u}_{i-1}}{h^2} \\ \underline{u}''(\theta_i) = f(\theta_i, \underline{u}(\theta_i), \underline{u}'(\theta_i)) \leftrightarrow \frac{\underline{u}_{i+1}-2\underline{u}_i+\underline{u}_{i-1}}{h^2} = f(\theta_i, \underline{u}_i, \frac{\underline{u}_{i+1}-\underline{u}_{i-1}}{2h}) \\ h = \frac{2\pi}{N} \end{cases} \tag{25}$$

Thus, we obtain $3N$ equations with $3N$ variables. The resolution of the system is achieved using the Newton method.

4 Validation of the model

The validation of the model is achieved by comparisons with Abaqus simulations. We'll compare first the nonlinear static deformations resulting from the application of vehicle load and inflation pressure and also the eigenmodes and transfer functions in the dynamic case. The same discretization is used in both Matlab and Abaqus simulations. A rigid wheel is considered in all the application cases which imply that each radial and tangential spring, representing the tire sidewalls, is connected to the ring at one extremity and embedded at the other one. The cross section is assumed to be rectangular with two dimensions *(b,e)*.The parameters used for the ring model are summarized in Table 1.

In the Abaqus model, the stiffness of radial and tangential springs, applied at each node, are calculated by the following formula:

$$k_R^{num} = Rd\theta k_R = \frac{2\pi R}{N}k_R \qquad k_\theta^{num} = Rd\theta k_\theta = \frac{2\pi R}{N}k_\theta \tag{26}$$

where N is number of nodes of the model.

Ring parameter	Description	Value
R	Tire radius	$0.32\ m$
e	Treadband thickness	$0.015\ m$
b	Treadband width	$0.12\ m$
k_R	Stiffness of radial spring	$3.0\ 10^6\ N/m$
k_θ	Stiffness of tangential spring	$4.73\ 10^4\ N/m$
E	Young Modulus	$3.2\ 10^8\ N/m^2$
ρ	Density	$1500\ kg/m^3$
ν	Poisson ratio	0.45
η	Structural damping	0.07

Table 1: Parameters of the proposed ring model

4.1 Static case

First, only the air pressure p is applied on the tire. In this case, the tangential displacement is zero and the radial displacement is constant along the beam because of the symmetry of the model. Moreover, on the cross-section, there is only normal strain. So it remains perpendicular to its neutral axis. The analytic formula of the radial displacement of the beam is the same in both Timoshenko and Euler Bernoulli cases:

- Linear case: $u^L = p\left(\frac{EA}{R^2} + \frac{EI}{R^4} + k_R\right)^{-1}$
- Nonlinear case: $\frac{1}{2}\left(\frac{EA}{R^3} + \frac{EI}{R^5} + 2\frac{k_R}{R}\right)\left(u^{NL}\right)^2 + \left(\frac{EA}{R^2} + \frac{EI}{R^4} + k_R - \frac{p}{R}\right)u^{NL} - p = 0$

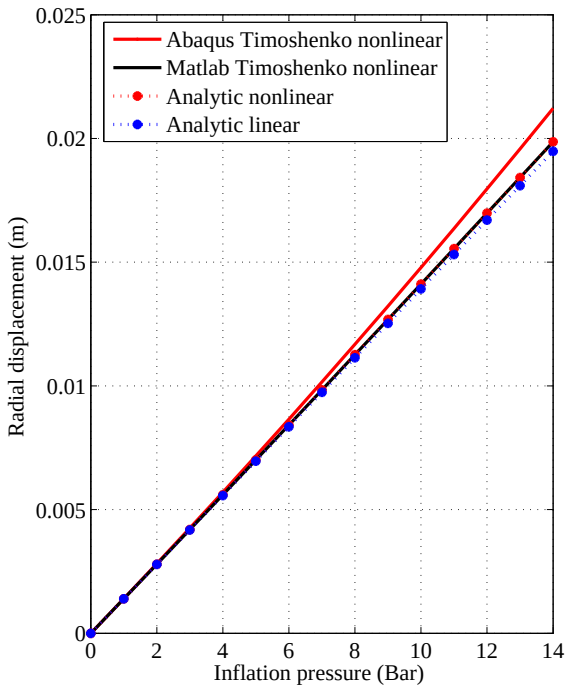

Figure 3: Radial displacement of the ring as function of the inflation pressure

The results obtained by these two analytical expressions are compared with nonlinear simulations performed in Matlab and Abaqus in Figure 3. When the inflating pressure is below $4.10^5\ Pa$, we see that all curves are

superposed. However, for more important values of pressure, a gap between the radial displacements computed in Abaqus and the other curves is observed. It can be explained by the assumption of no deformation in the cross section used in the construction of the proposed model. This is not the case with nonlinear Abaqus simulations. Consequently, the model is validated when the deformation of the beam remains small and the air pressure is below $6.10^5\ Pa$.

Secondly, besides an inflation pressure of $2.5\ 10^5\ Pa$, a punctual force of $2500\ N$ is added at the bottom of the tire representing the contact with the road. This is represented by a nodal force in the Matlab and Abaqus simulations. We compare the deformation shapes in the case of geometrical nonlinearity in Figure 4 which shows a good agreement of the results.

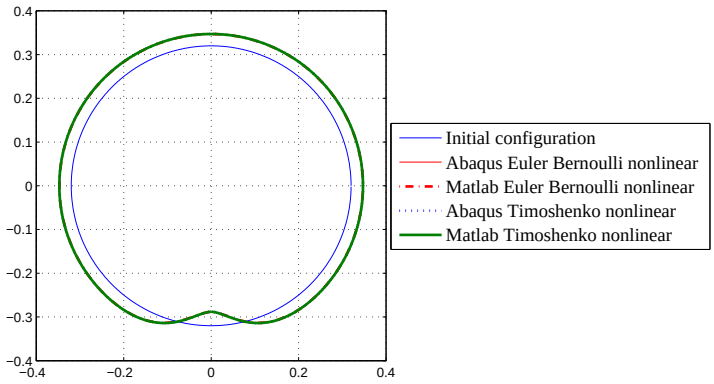

Figure 4: Undeformed vs. deformed shapes of the tire resulting from nonlinear static simulations

Figure 5 shows a comparison of linear and nonlinear deformed shapes of the tire.We can see that the difference is mostly located around the excited point. However, away from this point, the shapes are the same.

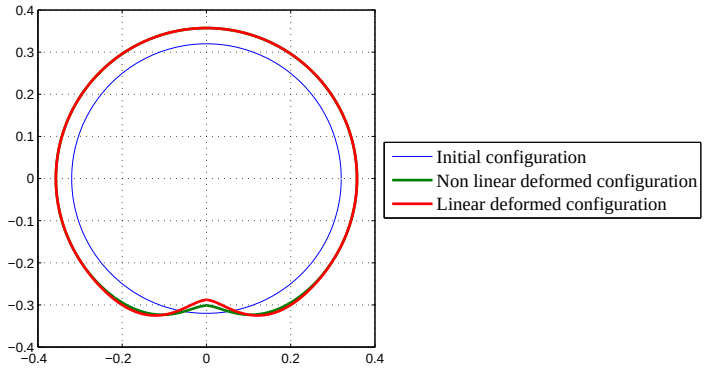

Figure 5: Comparison of linear and nonlinear deformed shapes of the tire

4.2 Dynamic case

We compare the natural frequencies of the tire around its nonlinear deformed shape. Two different boundary conditions are considered: fixed center and free basis (Figure 6, n being the circumferential wave number)

and both center and basis fixed (Figure 7). The results obtained by Matlab and Abaqus are very close. The errors are less than 1.2% what is very satisfactory.

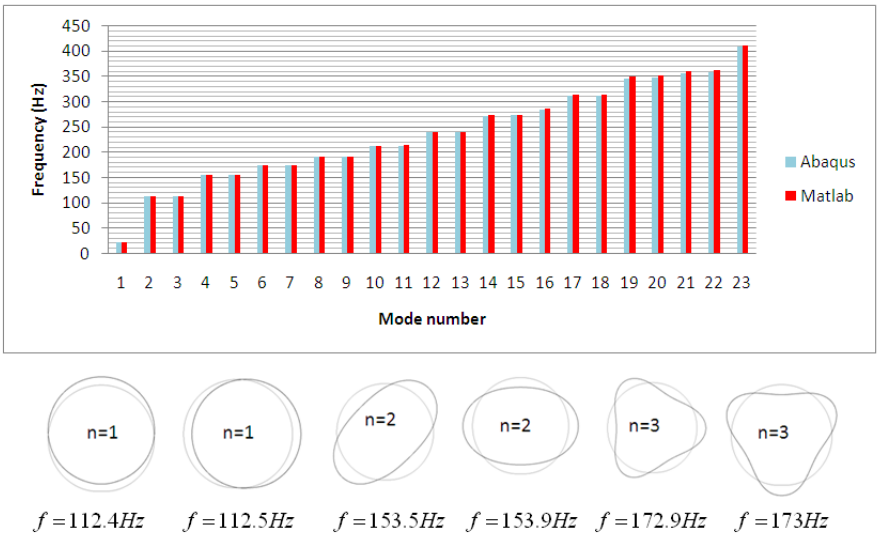

Figure 6: Tire eigenmodes with a fixed centre and a free base tire

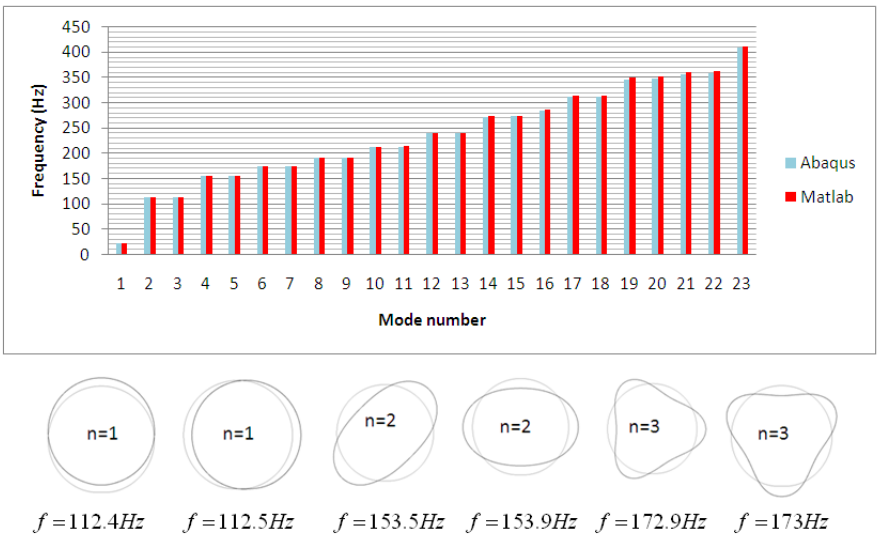

Figure 7: Tire eigenmodes with both centre and base fixed

An example of transfer function is depicted in Figure 8. It corresponds to the vertical reaction force at tire's centre resulting from a broadband vertical load applied on the tire basis with a constant amplitude equal to unity. The vertical reaction force is calculated as follows:

$$R_y = \int_0^{2\pi} k_R u_t . \left(\underline{u}_R, \underline{y}\right) d\theta + \int_0^{2\pi} k_\theta w_t . \left(\underline{u}_\theta, \underline{y}\right) d\theta \tag{27}$$

where $(,)$ denotes the $\Re^2$ scalar product.

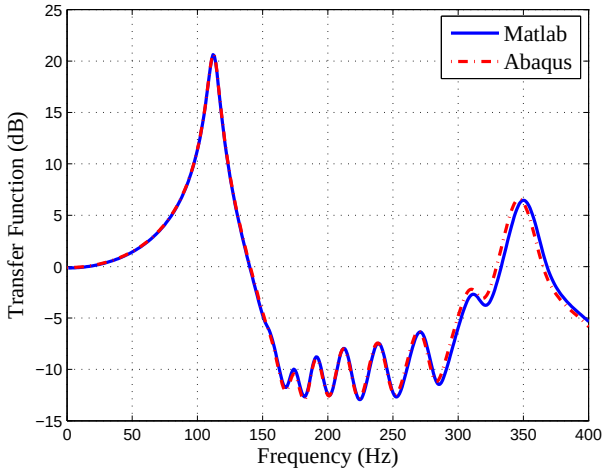

Figure 8: Vertical reaction force at the centre of the tire submitted to a unitary vertical load applied at its basis

The Matlab and Abaqus curves are superposed up to $300Hz$ and present small differences around $350Hz$ because the frequencies computed in Matlab and Abaqus are slightly different, for instance $f_{20} = 346Hz$ in Abaqus and $350Hz$ in Matlab (Figure 6). The difference remains very small. We obtain a good agreement between Matlab and Abaqus results.

5 Conclusion

This paper presents a 2D ring model for the analysis of tire dynamic behaviour under the load of a vehicle and an inflating pressure. The assumption of Timoshenko beam and finite displacements are considered to build the model. Thus, large rotations of the cross section and high order of translation displacements are taken into account but the cross section is assumed to remain undeformed. The analytical formulation is established successfully in linear/nonlinear static and dynamic states. We show that the simpler case of Euler Bernoulli's beam can be found from the more general equations of the model using Timoshenko's beam. In some special cases, we confirm their agreement with the equations found in the literature.
Since the nonlinear problem cannot be solved analytically, a numerical resolution method is proposed. The comparison with Abaqus simulations considered as reference allows the validation of the model. In the static case, we check that the deformed shapes are similar. In the dynamic case, we verify that the eigenmodes and transfer functions computed around the static state are in good agreement. These comparisons are performed for both Euler Bernoulli and Timoshenko beams in order to highlight the difference between the two formulations.
The proposed model can be extended for 3D analysis introducing all the lateral deformation and consequently the longitudinal moment effect at the tire centre. The rotation effects can also be applied to predict the dynamic behaviour in rolling conditions, for instance the frequency shifts with velocity.

References

[1] V. F. Böhm, *Mechanik des guertelreifens*, Ing-Arch (1966), pp. 35-82.

[2] F. Davi, *The theory of Kirchhoff rods as an exact consequence of three-dimensional elasticity*, Journal of Elasticity, Vol. 29 (1992), pp. 243-262.

[3] D. Duhamel, P. Campanac, K. Nonami, *Application of the vibration analysis of linear systems with time-periodic coefficients to the dynamics of rolling tire*, Journal of Sound and Vibration (2000), Vol. 231(1), pp. 37-77.

[4] Y. J. Kim, J. S. Bolton, *Effects of rotation on the dynamics of a circular cylindrical shell with applications to tire vibration*, Journal of Sound and Vibration (2003), Vol. 275(3-5), pp. 605-621.

[5] P. Kindt, P. Sas, W. Desmet, *Three-dimensional ring model for the prediction of the tire structural dynamic behaviour*, International Conference on Noise and Vibration Engineering, Leuven (2008), pp. 4155-4170.

[6] M. Muggleton, B. R. Mace, and M. J. Brennan, *Vibrational response prediction of a pneumatic using an orthotropic two-plate wave model*, Journal of Sound and Vibration (2003), Vol. 264, pp. 929-950.

[7] J. C. Simo, L. Vu-Quoc, *A finite strain beam formulation. The three dimensional dynamic problem*, Part I, Computer Methods in Applied Mechanics and Engineering (1985), Vol. 49, pp. 55-70.

[8] J. C. Simo, L. Vu-Quoc, *A three dimensional finite strain rod model*, Part II, Computer Methods in Applied Mechanics and Engineering (1986), Vol. 58, pp. 55-70.